

## In situ (Mg<sub>2</sub>Si+MgO)/Mg composites fabricated from AZ91-Al<sub>2</sub>(SiO<sub>3</sub>)<sub>3</sub> with assistance of high-energy ultrasonic field

ZHANG Song-li(张松利), ZHAO Yu-tao(赵玉涛), CHEN Gang(陈刚)

School of Materials Science and Engineering, Jiangsu University, Zhenjiang 212013, China

Received 23 October 2009; accepted 6 September 2010

**Abstract:** In situ (Mg<sub>2</sub>Si+MgO)/Mg composites fabricated from AZ91-Al<sub>2</sub>(SiO<sub>3</sub>)<sub>3</sub> under high-energy ultrasonic field were investigated by XRD, DSC and SEM. The results indicate that the size, morphology and distribution of the in situ Mg<sub>2</sub>Si particles are greatly optimized with the assistance of the high-energy ultrasonic field. The amounts of the in situ Mg<sub>2</sub>Si particles are increased, the sizes are refined, the distributions become uniform, and the morphologies are changed to smooth olive-shape or spherical shape. The amounts of brittle  $\beta$ -Mg<sub>17</sub>Al<sub>12</sub> phases are decreased and the morphologies are granulated. The values of the tensile strength  $\sigma_b$  and HB hardness are increased. These are due to the cavitation effects and acoustic streaming effects induced by the high-energy ultrasonic field.

**Key words:** in situ composites; high-energy ultrasonic field; morphology; microstructure; mechanical property

### 1 Introduction

Magnesium matrix composites reinforced by particles are attractive to meet the increasing demands of advanced structural applications, e.g. automotive and aerospace systems, due to their low density, high specific stiffness, high specific strength and good thermal stability compared with pure magnesium and their alloys[1–3]. The reinforcements can be classified as ex-situ and in-situ particles according to their source in the matrix[4]. In ex-situ particles reinforced magnesium matrix composites, the particles are added into the melt from the outside, such as liquid ingot casting and powder metallurgy; in in-situ particles reinforced magnesium matrix composites, the particles are formed within the melt, such as exothermic dispersion, reactive hot pressing, self-propagating high temperature synthesis, reactive infiltration and direct melt reactions[5–8]. As for the in-situ synthesis technology, the reinforcement particles are fabricated by chemical reactions and grow up in magnesium melt. These lead to neat particle/matrix interface, good wetting ability and high interface bonding strength. Especially, the direct melt reaction is considered one of the most potential and promising

techniques for commercial applications due to its simplicity, low cost and near net-shape forming capability[9].

In the present work, the mechanical effects, cavitation effects and acoustic streaming effects induced by the high-energy ultrasonic field on the microstructures and mechanical properties of the in situ Mg<sub>2</sub>Si/Mg composites fabricated from AZ91-Al<sub>2</sub>(SiO<sub>3</sub>)<sub>3</sub> are focused on. And the effects of the high-energy ultrasonic field on the in situ Mg<sub>2</sub>Si particles and microstructures of the magnesium alloy matrix are discussed in detail.

### 2 Experimental

The starting materials are commercial AZ91 ingots (Al 8.78, Zn 0.65, Mn 0.19, Fe 0.001 1, Cu 0.007 9, Si 0.045 5, Ni 0.000 8, Be 0.000 9, Cl 0.001 and Mg balance, mass fraction, %) and Al<sub>2</sub>(SiO<sub>3</sub>)<sub>3</sub> salt (AS881). Firstly, the Al<sub>2</sub>(SiO<sub>3</sub>)<sub>3</sub> salts were dehydrated at 250 °C for 3 h in an electric furnace. The AZ91 alloy ingots were heated at 5 °C/min in graphite crucible ( $d$ 100 mm $\times$ 240 mm) in an electric furnace under CO<sub>2</sub> and SF<sub>6</sub> gaseous mixture protection. When the temperature of the melt reached 720 °C, the dehydrated Al<sub>2</sub>(SiO<sub>3</sub>)<sub>3</sub> powder were added and pressed into the magnesium melt with a

**Foundation item:** Project(20070299004) supported by the Specialized Research Fund for the Doctoral Program of Higher Education of China; Project(BG2007030) supported by High-tech Research Program of Jiangsu Province, China; Projects(07KJA43008, 10KJD430003) supported by Natural Science Foundation of Jiangsu Province, China

**Corresponding author:** ZHAO Yu-tao; Tel: +86-511-88797658; E-mail: [zsl@ujs.edu.cn](mailto:zsl@ujs.edu.cn), [zhaoyt@ujs.edu.cn](mailto:zhaoyt@ujs.edu.cn)  
DOI: 10.1016/S1003-6326(09)60424-6

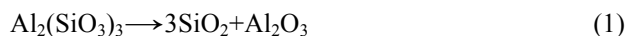
campanulate graphite mantle. After 10 min, a cylindrical amplitude lever was immersed into the magnesium about 5 mm in depth. The ultrasonic generation system was turned on. After 10 min high-energy ultrasonic operation, the magnesium melt was degassed, slag removed and refined. The magnesium melt was rested for 3 min and then was poured into a copper mould. After being cooled to the room temperature in air, the composite ingot was processed as the testing specimens.

X-ray diffractometer (Dmax2500PC) using Cu K<sub>α</sub> radiation was used to determine the phase component of the as-prepared specimens. Optical microscope (LAICA DM2500M) and scanning electron microscope (JEOL, JSM-7001F) were used to analyze the microstructures. Tensile properties of the specimens were tested at room temperature by a computer-controlled electronic tensile testing machine (DWD-200) at a strain rate of 1.67×10<sup>-4</sup> s<sup>-1</sup>. The tensile properties are the average values of three tests under each condition.

### 3 Results and discussion

#### 3.1 Phase components

Fig.1 shows XRD pattern of the as-prepared composites fabricated with assistance of high-energy ultrasonic. As shown in Fig.1, Mg, Mg<sub>2</sub>Si, Mg<sub>17</sub>Al<sub>12</sub> and MgO phases are observed according to Ref.[10–13]. In Mg-Al<sub>2</sub>(SiO<sub>3</sub>)<sub>3</sub> system, some chemical reactions take place in the molten magnesium liquid according to the XRD and thermodynamics calculations results. The formations of the in-situ reinforcement phases in experiments are described as follows. In magnesium melt, the Al<sub>2</sub>(SiO<sub>3</sub>)<sub>3</sub> salt are decomposed to SiO<sub>2</sub> and Al<sub>2</sub>O<sub>3</sub> according to the following reaction:



Then, SiO<sub>2</sub> and Al<sub>2</sub>O<sub>3</sub> can react with magnesium according to the following two reactions:

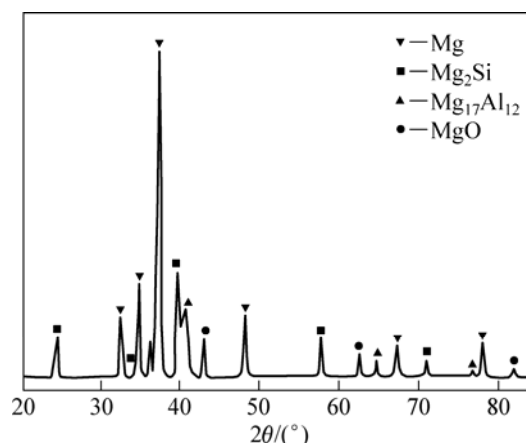


Fig.1 XRD patterns of as-prepared composites fabricated with assistance of high-energy ultrasonic field



The possibility of Eqs.(2) and (3) was determined by the Gibbs free energy values calculated from thermodynamics.

As for  $n_1A_1 + n_2A_2 = n_3A_3 + n_4A_4$  type chemical reaction system, the reaction free energy can be calculated as

$$\Delta H_T = \Delta H_{298} + \int_{298}^{T_m} \Delta c_{p(1)} dT + \Delta H_m + \int_{298}^T \Delta c_{p(2)} dT \quad (4)$$

$$\Delta S_T = \Delta S_{298} + \int_{298}^{T_m} \frac{\Delta c_{p(1)}}{T} dT + \frac{\Delta H_m}{T_m} + \int_{298}^T \frac{\Delta c_{p(2)}}{T} dT \quad (5)$$

$$\Delta G_T = \Delta H_T - T\Delta S_T \quad (6)$$

where  $\Delta c_p = n_3\Delta c_{p(3)} + n_4\Delta c_{p(4)} + n_1\Delta c_{p(1)} + n_2\Delta c_{p(2)}$ .

For simplifying the calculations, Eqs.(4)–(6) can be written as the following linear equation:

$$\Delta G_T = a + bT \quad (7)$$

The thermodynamic parameters of the elements and compounds are listed in Table 1.

According to Ref.[14], the free energy parameters

Table 1 Thermodynamics parameters of elements and compounds[14]

| Substance                      | $c_p/(4.2 \text{ J}\cdot\text{mol}^{-1}\cdot\text{K}^{-1})$ |          |             | $\Delta H_{298}/$<br>(4.2 kJ·mol <sup>-1</sup> ) | $\Delta S_{298}/$<br>(4.2 kJ·mol <sup>-1</sup> ·K <sup>-1</sup> ) | $T_m/\text{K}$ | $\Delta H_m/$<br>(4.2 kJ·mol <sup>-1</sup> ) |
|--------------------------------|---|----------|-------------|--|---|----------------|--|
|                                | $a$   | $b/10^3$ | $c/10^{-5}$ |  |   |                |  |
| Mg(s)                          | 5.33  | 2.45     | -0.103      | 0  | 7.81  | 872            | 2.14   |
| Mg(l)                          | 7.80  | -        | -           | -  | -   | -              | -  |
| SiO <sub>2</sub>               | 10.49   | 0.24     | -1.44       | -217.6   | 9.91  | 1722           | 1.84   |
| MgO                            | 11.71   | 0.75     | -2.80       | -143.7   | 6.44  | 2825           | 18.5   |
| Mg <sub>2</sub> Si             | 17.52   | 3.58     | -2.11       | -18.9  | 15.25   | 1077           | 20.5   |
| Si                             | 5.72  | 0.59     | -0.99       | 0  | 4.5   | 1685           | 12.0   |
| Al <sub>2</sub> O <sub>3</sub> | 27.3  | 3.05     | -8.44       | -397.4   | 12.1  | 2723           | 26.0   |
| Al                             | 4.94  | 2.96     | -           | 0  | 6.77  | 933            | 2.6  |

\*  $c_p = a + bT + cT^2 + dT^3$

of the reactions (2) and (3) are as follows, respectively:

$$\Delta G_T(2) = 100\,500 + 17.2T \quad (8)$$

$$\Delta G_T(3) = -378\,00 + 9.3T \quad (9)$$

When the melt temperature is 993 K,  $\Delta G_T(2) = -83\,420$  kJ/mol, and  $\Delta G_T(3) = -28\,565.1$  kJ/mol. This means that the reactions (2) and (3) can take place spontaneously in the above conditions. The results of the thermodynamic calculations are in concordance with the XRD results.

### 3.2 Microstructures

Fig.2 shows the SEM images of the as-prepared composites synthesized from AZ91-Al<sub>2</sub>(SiO<sub>3</sub>)<sub>3</sub> system without and with the assistance of the ultrasonic field. It can be clearly seen that, with ultrasonic field, the in situ Mg<sub>2</sub>Si and MgO particles are distributed and dispersed uniformly in the magnesium matrix, and Mg<sub>17</sub>Al<sub>12</sub> are dispersed in macro-scale. The morphologies of the in situ Mg<sub>2</sub>Si particles are presented in near spherical shape or smooth quadrangle-shape with size of about 2–3 μm, MgO particles in spherical shape with size of about 0.1–0.5 μm, and the Mg<sub>17</sub>Al<sub>12</sub> intermetallic compound in massive shape, bone-shape, or long strip-shape, due to the effects of the high-energy ultrasonic field.

The cavitation effect of the high-power ultrasonic field is due to the expanding–clogging–bursting dynamical processing for the ultrasonic bubbles. When the high-power ultrasonic field is transmitted to the

magnesium melt, the melt bears the tensile stress and the cavitations are born. Then, the cavitations are rapidly expanded, clogged and burst in the magnesium melt. The instantaneous local high-temperature, high press and intensive blast wave are thus created[15] and greatly contributed to the crack and peripheral-smooth for the bonding net-shape Mg<sub>2</sub>Si phases and brittle Mg<sub>17</sub>Al<sub>12</sub> phases.

When the high-power ultrasonic field is transmitted to the aluminum melt, the sonic press gradients are built from the sonic source due to the finite amplitude attenuation of the interaction of the sound wave and the viscous force of the magnesium melt. These sonic press gradients are contributed to the flowing of the melt and the circulation flow in the magnesium melt. The flowing direction of the melt under the amplitude lever is vertical-downward, and the flowing speed is fast. After reaching the bottom of the crucible and reversely moving upward, the flowing speed is reduced. The spiral vortex is formed near the end face of the amplitude lever. These induce the acoustic streaming effects: vibration and stirring.

The above effects of the high-energy ultrasonic field contribute to the diffusion of the reactants and the products. Thus, the in situ chemical reactions are speeded and the broken Mg<sub>2</sub>Si and Mg<sub>17</sub>Al<sub>12</sub> phases distribute uniformly in the magnesium melt.

### 3.3 Mechanical properties

The mechanical properties of the composites fabricated without and with the assistance of ultrasonic field are listed in Table 2. It is indicated that with the assistance of the high-energy ultrasonic field, the values of the tensile strength and HB hardness are increased. The tensile strength  $\sigma_b$ , HB hardness and elongation  $\delta$  are 276.24 MPa, 83.49 MPa and 3.97%, which are 1.42, 1.35 and 1.13 times those of without the assistance of the high-energy ultrasonic field, respectively.

**Table 2** Mechanical properties of composites fabricated with and without assistance of ultrasonic field

| Ultrasonic field | Tensile strength/MPa | Elongation/% | Brinell hardness/MPa |
|------------------|----------------------|--------------|----------------------|
| Without          | 194.53               | 3.51         | 61.84                |
| With             | 276.24               | 3.97         | 83.49                |

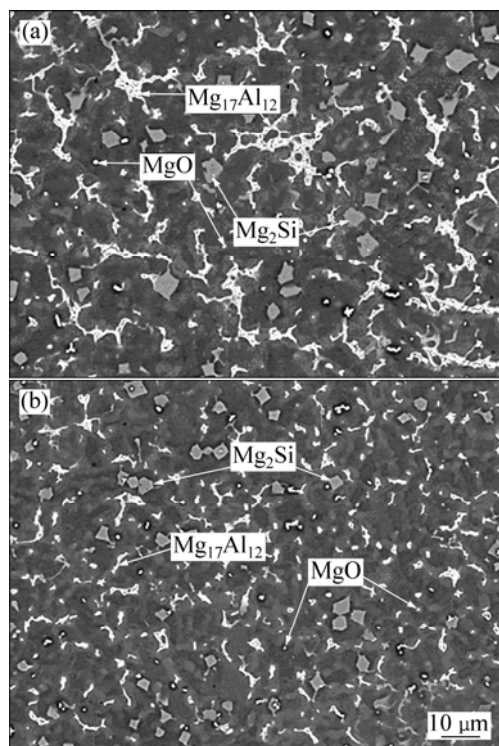


**Fig.2** SEM images of composites synthesized from AZ91-Al<sub>2</sub>(SiO<sub>3</sub>)<sub>3</sub> system without (a) and with ultrasonic field assistance (b)

Fig.3 gives the SEM images of the tensile fracture surface of the tested specimens. It can be clearly seen that the appearances of the fracture surfaces are different in size and depth with and without ultrasonic field. As shown in Fig.3(a), the tensile fracture surface shows the obvious cleavage fracture characteristics, the brittle  $\beta$ -Mg<sub>17</sub>Al<sub>12</sub> phases are clearly seen on the fracture surface and become the main crack nucleating site, and

the observed dimples are shallower in depth and larger in size and parts are linked along the boundaries. With ultrasonic field, the brittle  $\beta$ -Mg<sub>17</sub>Al<sub>12</sub> and Mg<sub>2</sub>Si phases are refined, the ratio of the surface area to volume is increased, and the surface tension is increased. These hinder the expansion of the deformed area along the boundary of the crystal grain. As shown in Fig.3(b), the observed dimples are deeper in depth and smaller in size. The appearances of the tearing deformation inside the crystal are clearly observed, and the cleavage fracture characteristics are weakened. The fracture mechanisms are the plastic fracture and cleavage fracture.

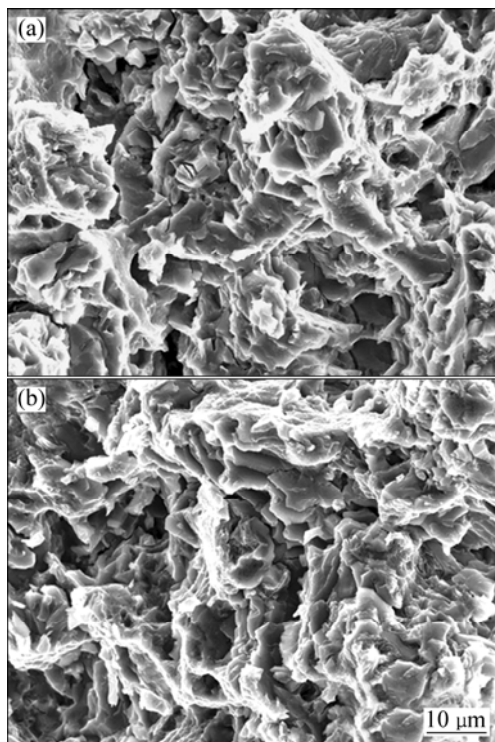


**Fig.3** SEM images of tensile fracture surface of composites synthesized from AZ91-Al<sub>2</sub>(SiO<sub>3</sub>)<sub>3</sub> system without (a) and with (b) ultrasonic field assistance

## 4 Conclusions

1) In situ (Mg<sub>2</sub>Si+MgO)/Mg composites are fabricated from AZ91-Al<sub>2</sub>(SiO<sub>3</sub>)<sub>3</sub> with the assistance of the high-energy ultrasonic field.

2) The sizes, morphologies and distributions of the in situ Mg<sub>2</sub>Si particles are more greatly optimized with high-energy ultrasonic field than those without high-energy ultrasonic field. Under the ultrasonic field, the amounts of the in situ Mg<sub>2</sub>Si particles are increased, the sizes are refined, the distribution becomes uniform, and the morphologies are changed to smooth olive-shape or spherical shape. The amounts of brittle  $\beta$ -Mg<sub>17</sub>Al<sub>12</sub>

phases are decreased and the morphologies are granulated.

3) The values of the tensile strength  $\sigma_b$  and HB hardness are increased, reaching 276.24 MPa and 83.49 MPa, respectively.

## References

- [1] ZHENG Ming-yi, WU Kun, YAO Cong-kai. Effect of interfacial reaction on mechanical behavior of SiCw/AZ91 magnesium matrix composites [J]. *Materials Science and Engineering A*, 2001, 318(1/2): 50–56.
- [2] WANG Xiao-feng, ZHAO Jiu-zhou, HE Jie, HU Zhuang-qi. Hot rolling characteristics of spray-formed AZ91 magnesium alloy [J]. *Transactions of Nonferrous Metals Society of China*, 2007, 17(2): 238–243.
- [3] YE Hai-zhi, LIU Xing-yang. Review of recent studies in magnesium matrix composites [J]. *Journal of Materials Science*, 2004, 39(20): 6135–6171.
- [4] IBRAHIM IA, MOHAMED FA, LAVERNIA E J. Particulate reinforced metal matrix composites—A review [J]. *Journal of Materials Science*, 1991, 26(5): 1137–1156.
- [5] UMEDA J, KONDOH K, IMAI H. Friction and wear behavior of sintered magnesium composite reinforced with CNT-Mg<sub>2</sub>Si/MgO [J]. *Materials Science and Engineering A*, 2009, 504(1/2): 157–162.
- [6] SHYU R F, HO C T. In situ reacted titanium carbide-reinforced aluminum alloys composite [J]. *Journal of Materials Processing Technology*, 2006, 171(3): 411–416.
- [7] WANG X J, WU K, HUANG W X, ZHANG H F, ZHENG M Y, PENG D L. Study on fracture behavior of particulate reinforced magnesium matrix composite using in situ SEM [J]. *Composites Science and Technology*. 2007, 67(11/12): 2253–2260.
- [8] YAN Wei-ping, RONG Fu-jie, SONG Guo-jin, ZHAI Hu, MA Zhi-yi, FENG Zhi-jun. Present status of studying of TiB<sub>2</sub>/Al composite fabricated by mixed salts method [J]. *Foundry*, 2006, 55(11): 1114–1117. (in Chinese)
- [9] DONG Long-xiang, WU Yao-ming, DOU Chuan-guo, XU Guo-gen, WANG Li-min. Structural characterization and property of in-situ synthesized AZ91-Mg<sub>2</sub>Si composite [J]. *Transactions of Nonferrous Metals Society of China*, 2006, 16(z3): 1845–1847.
- [10] AMBAT R, AUNG N, ZHOU W. Evaluation of microstructural effects on corrosion behaviour of AZ91D magnesium alloy [J]. *Corrosion Science*, 2000, 42(8): 1433–1455.
- [11] OWEN E A, PRESTON G D. The atomic structure of two intermetallic compounds [J]. *Proceedings of the Physical Society of London*, 1923, 35(2): 341–348.
- [12] SCHOBINGER-PAPAMANTELLOS P, FISCHER P. Neutronenbeugungsuntersuchung der atomverteilung von Mg<sub>17</sub>Al<sub>12</sub> [J]. *Naturwissenschaften*, 1970, 57(3): 128–129.
- [13] BIRKS L S, FRIEDMAN H. Particle size determination from X-ray line broadening [J]. *Journal of Applied Physics*, 1946, 17(8): 687–692.
- [14] HU Yong, YAN Hong, CHEN Guo-xiang. Thermodynamics and kinetics of in-situ synthesized Mg<sub>2</sub>Si/AM60 composites [J]. *Special Casting & Nonferrous Alloys*, 2008, 28(3): 239–242. (in Chinese)
- [15] FENG Ruo, LI Hua-mao. *Phonochemistry and its applications* [M]. Hefei: Anhui Science and Technology Publication House, 1990. (in Chinese)

(Edited by YANG Bing)